STUDIES OF THE ROPER RESONANCE BY THE LJUBLJANA GROUP*

Simon Širca

Faculty of Mathematics and Physics, University of Ljubljana, Slovenia
and
Jožef Stefan Institute, Ljubljana, Slovenia

Received 28 October 2025, accepted 31 October 2025, published online 10 February 2026

Ever since its discovery in 1964, the nature of the $N^*(1440)$ nucleon resonance has been a perpetual and one of the outstanding puzzles in hadronic physics. The Ljubljana group joined the global effort in the late 1990s, first from the theoretical viewpoint and later experimentally. This paper is a short overview of our attempts to understand this elusive resonance.

DOI:10.5506/APhysPolB.57.2-A9

1. Introduction

The first excited state of the nucleon with the same quantum numbers, the $N^*(1440)$ or the "Roper" resonance [1], has evaded detailed understanding by the hadronic community for decades. One of the reasons is that it is anything but conspicuous, being hidden below much more prominent neighboring resonances, in particular the $\Delta(1232)$ (P_{33}) and the $N^*(1520)$ (D_{13}) which were already known at the time of the discovery, possessing an unusually large width and exhibiting a very atypical behavior of $\mathrm{Im}\, T_{\pi N}$ in the P_{11} partial wave. Indeed, Professor L.D. Roper himself appeared to be reluctant to accept the rather peculiar feature in the Argand diagram and, as quoted in [2], lamented: "I spent [a] much time trying to eliminate the P_{11} resonance." The progress brought about by partial-wave analyses was not as fast as one would hope for and did not converge well, and I can still recall Professor Arndt's response at the 2004 conference at ACU to a question on how one could best improve the determination of the P_{11} mass(es?), width, pole position, and decay properties. It was indicative of the issues that the partial-wave community was facing: "I've expressed my position on this subject many times. It just isn't possible to fit P_{11} with a 'simple' Breit–Wigner form; the amplitude is determined by nearby singularities consisting of two poles and a very prominent cut (π–Δ). It's like doing a polynomial fit to a sine wave. [...] I believe that the 'problem' with P_{11} is that people keep trying to stuff a square pole in a round hole."

* Funded by SCOAP[3] under Creative Commons License, CC-BY 4.0.

As members of two hadron-physics groups from the Jožef Stefan Institute and the Faculty of Mathematics and Physics in Ljubljana, Slovenia, consisting of Professor Mitja Rosina, late Professor Bojan Golli, and the Author, we were motivated to investigate the Roper resonance partly due to our existing know-how in statical and dynamical properties of the nucleons studied in terms of quark models. These model calculations, initially performed in collaboration with our Portuguese colleagues from Coimbra (J. da Providência, J. Urbano, M. Fiohais, and P. Alberto), were initiated even prior to that, and were thriving on an earlier substrate of the Peierls–Yoccoz projection technique, coherent states, and the "hedgehog" ansatz for the baryon wave functions [3].

2. The Roper resonance in the chromodielectric model

Our first attempt at explaining a specific feature of the Roper resonance in terms of a quark model was to calculate the transverse and scalar helicity amplitudes for the nucleon–Roper transition, $A_{1/2}$ and $S_{1/2}$. The Roper resonance was described in a chiral version of the chromodielectric model (CDM) as consisting of a three-quark core with one of the quarks promoted to the $2s$ orbit, surrounded by a cloud of pions and σ-mesons, and furnished with a chromodielectric field χ which ensures that the quarks remain dynamically confined [4]. The χ field is a peculiar ingredient of the CDM, and this feature of the model has also been relevant in other contexts, in particular in quantifying the role of the pion cloud, that is, "counting pions in the nucleon" [5].

The wave functions of the physical nucleon and the Roper resonance were obtained by performing the Peierls–Yoccoz projection on the baryon wave function in the form of a "hedgehog" coherent state and making them orthogonal to one another. The Roper resonance was represented as a breathing mode of the three valence quarks in the bare core (the source), with all three meson fields adapting to the changes in the source; all fields were computed in a self-consistent manner. (Alternatively, the Roper could be modeled by retaining all three core quarks in the ground state but letting the χ field and/or the σ field oscillate.) We have computed the Q^2 dependence of the helicity amplitudes $A^p_{1/2}$ and $S^p_{1/2}$ in the range of $0 \leq Q^2 \leq 2$ $(\mathrm{GeV}/c)^2$ and obtained correct signs and reasonable trends at a time when the world data consisted merely of three points with unspecified (possibly huge) uncertainties which, moreover, were at odds with the rather accurately determined helicity couplings at $Q^2 = 0$. We also computed $A^n_{1/2}(Q^2)$ for which the only experimental reference was at the photon point, missing it by a factor of approximately two.

3. Coupled-channel approach with chiral quark models

Since in the CDM the χ field takes care of the confinement, the accompanying pion field is accordingly weaker, resulting in a smaller average number of pions and, we presumed, in a relatively minor contribution of the pion cloud in the photo-excitation amplitudes. The abundance of theoretical and experimental studies of the N–Δ transition at the turn of the millennium — see, for instance, [6] and references therein for a review — provided ample evidence that the pion cloud indeed plays an important role, especially at small Q^2. This motivated us to open a much wider front and to construct a coupled-channel framework that would allow for the analysis of the electro-magnetic excitation parts of the photo- and electro-production processes as well as their strong decay parts. The framework that we devised [7] is in principle able to accommodate any underlying quark model, but we have chosen to perform all our calculations by using the Cloudy Bag Model (CBM), for the simple reason that the quark–meson interaction matrix elements were relatively easy to compute and, in addition, due to its presumed advantage of featuring a much stronger pion cloud than, say, the CDM.

In our coupled-channel K-matrix formalism, we only consider models in which the meson fields couple linearly to the quark core, and there is no meson self-interaction. The part of the Hamiltonian corresponding to mesons has the form

$$H_{\rm m} = \int {\rm d}k \sum_{lmt} \left\{ \omega_k \, a^\dagger_{lmt}(k) a_{lmt}(k) + \left[V_{lmt}(k) a_{lmt}(k) + V_{lmt}(k)^\dagger \, a^\dagger_{lmt}(k) \right] \right\} , \tag{1}$$

where $a^\dagger_{lmt}(k)$ is the creation operator for an l-wave meson with the third component of spin m and — in the case of isovector mesons — the third component of isospin t. In the case of the p-wave pions, the source can be cast in the form

$$V_{1mt}(k) = -v(k) \sum_{i=1}^{3} \sigma^i_m \tau^i_t \, , \tag{2}$$

with $v(k)$ depending on a particular quark model and containing the information about the underlying quark structure. Note that $V_{lmt}(k)$ may also induce radial excitations of the quark core, in particular $1s \to 2s$, $1s \to 1p_{1/2}$, and $1s \to 1p_{3/2}$ transitions. In the model of choice, CBM, the relevant operators are

$$V^{s\to s}_{1mt}(k) \;=\; \frac{1}{2f} \, \frac{k^2}{\sqrt{12\pi^2 \omega_k}} \, \frac{\omega_s}{\omega_s - 1} \, \frac{j_1(kR_{\rm bag})}{kR_{\rm bag}} \sum_{i=1}^{3} \sigma^i_m \tau^i_t \, ,$$

$$V_{1mt}^{s\to 2s}(k) = \frac{1}{2f}\frac{k^2}{\sqrt{12\pi^2\omega_k}}\sqrt{\frac{\omega_{2s}\omega_s}{(\omega_{2s}-1)(\omega_s-1)}}\frac{j_1(kR_{\rm bag})}{kR_{\rm bag}}\sum_{i=1}^{3}\sigma_m^i\tau_t^i\,,$$

$$V_{00t}^{s\to p_{1/2}}(k) = \frac{1}{f}\frac{k^2}{\sqrt{4\pi^2\omega_k}}\sqrt{\frac{\omega_{p_{1/2}}\omega_s}{(\omega_{p_{1/2}}+1)(\omega_s-1)}}\frac{j_0(kR_{\rm bag})}{kR_{\rm bag}}\sum_{i=1}^{3}\tau_t^i\,,$$

$$V_{2mt}^{s\to p_{3/2}}(k) = \frac{1}{2f}\frac{k^2}{\sqrt{2\pi^2\omega_k}}\sqrt{\frac{\omega_{p_{3/2}}\omega_s}{(\omega_{p_{3/2}}-2)(\omega_s-1)}}\frac{j_2(kR_{\rm bag})}{kR_{\rm bag}}\sum_{i=1}^{3}\Sigma_{2m}^i\tau_t^i\,,$$

involving p-wave, p-wave, s-wave, and d-wave pions, respectively.

The next step is to construct the K matrix. The idea is to include many-body states of quarks (and mesons) in the scattering formalism in a Chew–Low-type approach [8]. This is most easily accomplished in the JT basis in which the K and T matrices are diagonal. The K matrix has the form

$$K_{\pi N\pi N}^{JT}(k,k_0) = -\pi\sqrt{\frac{\omega_k E_N}{k\,W}}\,\langle\Psi_{JT}^N(W)|\,|V(k)||\Psi_N\rangle\,, \tag{3}$$

and we introduce the principal-value states

$$|\Psi_{JT}^N(W)\rangle = \sqrt{\frac{\omega_0 E_N}{k_0 W}}\left\{\left[a^\dagger(k_0)|\Psi_N\rangle\right]^{JT} - \frac{\mathcal{P}}{H-W}\,[V(k_0)|\Psi_N\rangle]^{JT}\right\}\,, \tag{4}$$

where $[\quad]^{JT}$ denotes coupling to good J and T, W is the invariant energy of the system, ω_0 and k_0 are the energy and momentum of the pion, and E_N is the nucleon energy.

This set of formulas has then been extended to the multi-channel case, assuming that two-pion decays proceed through some intermediate unstable particle, either a baryon or a meson, as shown in Fig. 1. The task at hand, then, was to devise principal-value states with suitable orthogonality

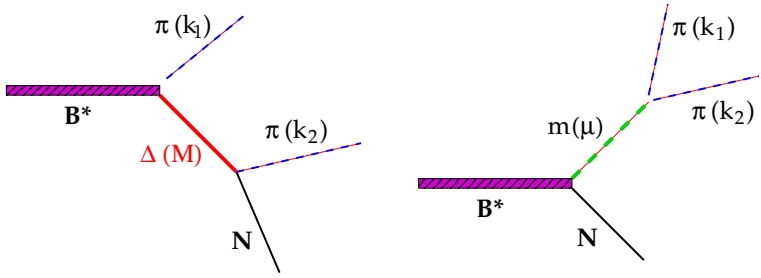

Fig. 1. Two-pion decay of an excited baryon involving an intermediate unstable baryon with the invariant mass M like the Δ (left) or an unstable meson with the invariant mass μ, for instance, the σ meson (right).

and normalization properties, and use them to construct a multi-channel K matrix with the general form

K_{NN}	$K_{NB}(M')$	$K_{N\sigma}(\mu')$
$K_{BN}(M)$	$K_{BB'}(M,M')$	$K_{B\sigma}(M,\mu')$
$K_{\sigma N}(\mu)$	$K_{\sigma B}(\mu,M)$	$K_{\sigma\sigma}(\mu,\mu')$

Once the K matrix is obtained, the T and S matrices are given by the relations

$$T = \frac{K}{1 - iK}\,, \qquad S = 1 + 2iT\,. \tag{5}$$

In integral form, the first equation in (5), $T = K + i\,TK$, amounts to the set of coupled integral (Heitler) equations

$$\begin{aligned}
T_{NN} &= K_{NN} + iT_{NN}K_{NN} \\
&\quad + i\sum_B \int_{M_N+m_\pi}^{W-m_\pi} \mathrm{d}M\, T_{NB}(M)K_{BN}(M) \\
&\quad + i \int_{2m_\pi}^{W-M_N} \mathrm{d}\mu\, T_{N\sigma}(\mu)K_{\sigma N}(\mu)\,, \\
T_{NB}(M) &= K_{NB}(M) + iT_{NN}K_{NB}(M) \\
&\quad + i\sum_{B'} \int_{M_N+m_\pi}^{W-m_\pi} \mathrm{d}M'\, T_{NB'}\left(M'\right) K_{B'B}\left(M', M\right) \\
&\quad + i \int_{2m_\pi}^{W-M_N} \mathrm{d}\mu\, T_{N\sigma}(\mu)K_{\sigma B}(\mu, M)\,, \\
T_{N\sigma}(\mu) &= K_{N\sigma}(\mu) + iT_{NN}K_{N\sigma}(\mu) \\
&\quad + i\sum_B \int_{M_N+m_\pi}^{W-m_\pi} \mathrm{d}M\, T_{NB}(M)K_{B\sigma}(M,\mu) \\
&\quad + i \int_{2m_\pi}^{W-M_N} \mathrm{d}\mu'\, T_{N\sigma}(\mu')K_{\sigma\sigma}(\mu',\mu)\,.
\end{aligned} \tag{6}$$

The desired principal-value states $|\Psi^B_{JT}(W,M)\rangle$ corresponding to the πB channel (where B stands for any intermediate baryon, for instance, the Δ)

were introduced in a form analogous to (4)

$$\left|\Psi^B_{JT}(W,M)\right\rangle = \mathcal{N}_1 \left\{ \left[a^\dagger(k_1)\left|\widetilde{\Psi}_B(M)\right\rangle\right]^{JT} - \frac{\mathcal{P}}{H-W}\left[V(k_1)\left|\widetilde{\Psi}_B(M)\right\rangle\right]^{JT}\right\}, \tag{7}$$

where $\widetilde{\ }$ signifies that orthonormality has been accounted for. The K-matrix elements computed with such states are

$$\begin{aligned}
K^{JT}_{\pi B\pi N}(k,k_0,M) &= -\pi\sqrt{\frac{\omega_k E}{k\,W}}\langle\Psi^N_{JT}(W)||V(k)||\,\widetilde{\Psi}_B(M)\rangle\,,\\
K^{JT}_{\pi N\pi B}(k,k_1,M) &= -\pi\sqrt{\frac{\omega_k E}{k\,W}}\langle\Psi^B_{JT}(W,M)||V(k)||\,\Psi_N\rangle\,,\\
K^{JT}_{\pi B'\pi B}\left(k,k_1,M',M\right) &= -\pi\sqrt{\frac{\omega_k E}{k\,W}}\langle\Psi^B_{JT}(W,M)||V(k)||\,\widetilde{\Psi}_{B'}\left(M'\right)\rangle\,,
\end{aligned}$$

describing, from top to bottom, a process in which the initial πN system with the invariant mass W decays into a pion and a πN system with the quantum numbers of the intermediate baryon B; the $\pi B\to\pi N$ transition; and the $\pi B\to\pi B'$ transition, for instance, $\pi(k_1)+\Delta(M)\to\pi(k)+\Delta(M')$. Similar expressions are derived for the channels involving the σ mesons. (For purposes of brevity and in tune with the scope of the paper, the lengthy expressions with a similar structure for different inelastic channels shall also be omitted in the following; consult [7] for details.)

One of the obstacles encountered was that in formal expressions such as (4) or (7), the interaction $V(k)$ generates bare three-quark states with quantum numbers different from the ground state, as well as superpositions of bare three-quark states dressed with mesons. This problem has been resolved by exploiting general expressions for the matrix elements of the pion field between the eigenstates of the Hamiltonian whose pion part has the form (1); see Appendix A of [7]. As an illustration, the elastic channel has been represented by the ansatz

$$\begin{aligned}
\left|\Psi^N_{JT}(W)\right\rangle &= \mathcal{N}_0\left\{\sum_{\mathcal{R}} c^N_{\mathcal{R}}(W)\,|\Phi_{\mathcal{R}}\rangle + \left[a^\dagger(k_0)\,|\Psi_N(k_0)\rangle\right]^{JT}\right.\\
&\quad + \int \mathrm{d}k\,\frac{\chi^{NN}_{JT}(k,k_0)}{\omega_k+E_N(k)-W}\left[a^\dagger(k)\,|\Psi_N(k)\rangle\right]^{JT}\\
&\quad + \sum_B\int \mathrm{d}M\int \mathrm{d}k\,\frac{\chi^{BN}_{JT}(k,k_0,M)}{\omega_k+E_B(k)-W}\left[a^\dagger(k)\left|\widetilde{\Psi}_B(M)\right\rangle\right]^{JT}\\
&\quad \left. + \int \mathrm{d}\mu\int \mathrm{d}k\,\frac{\chi^{\sigma N}_{JT}(k,k_0,\mu)}{\omega_{\mu k}+E_{JT}(k)-W}\,b^\dagger(k)\left|\widetilde{\Psi}_{JT}\right\rangle\right\}
\end{aligned} \tag{8}$$

with the following structure: the first term is the sum over bare quark states, denoted $\Phi_{\mathcal{R}}$; the second term corresponds to the unmodified (free) pion and defines the channel as well as determines the normalization; the three integral terms incorporating the meson-field amplitudes χ correspond to the meson-cloud contributions, specifically, to the one-pion state superposed on the ground state, to one-pion states around different excited states, and to the one-σ state around either the nucleon or the Δ, respectively. In an analogous manner, one can then construct the principal-value states for the inelastic channels, in particular $|\Psi^B_{JT}(W,M)\rangle$ for the πB channels, and $|\Psi^\sigma_{JT}(W,\mu)\rangle$ for the σN channel.

In the channels including the pion and unstable isobars, the meson amplitudes χ above the one- and two-pion thresholds are related to the elastic and inelastic elements of the K matrix,

$$\begin{aligned} K_{NN}(W) &= \pi\,\mathcal{N}_0^2\,\chi^{NN}_{JT}(k_0,k_0)\,, \\ K_{BN}(W,M) &= \pi\,\mathcal{N}_0\,\mathcal{N}_1\,\chi^{BN}_{JT}(k_1,k_0,M)\,, \\ K_{\sigma N}(W,\mu) &= \pi\,\mathcal{N}_0\,\mathcal{N}_\mu\,\chi^{\sigma N}_{JT}(k_\mu,k_0,\mu)\,, \end{aligned} \tag{9}$$

while above the two-pion threshold, the relations read

$$K_{H'H}\left(W,m'_H,m_H\right) = \pi\,\mathcal{N}_{H'}\mathcal{N}_H\,\chi^{H'H}_{JT}\left(k_{H'},k_H,m'_H,m_H\right)\,. \tag{10}$$

Here, H stands for either the πB or σN channels, and m_H is the corresponding invariant mass, M or μ, respectively.

Next, the equations for the pion amplitudes χ, the coefficient $c_{\mathcal{R}}$ in the ansatz (8), and the analogous coefficients $\widehat{c}^B_{\mathcal{R}}$ appearing in $|\Psi^B_{JT}(W,M)\rangle$ and $\widehat{c}^\sigma_{\mathcal{R}}$ appearing in $|\Psi^\sigma_{JT}(W,\mu)\rangle$, must be obtained. The appropriate equations can be derived by invoking the Kohn variational principle $\langle\delta\Psi^{\mathrm{P}}|H - W|\Psi^{\mathrm{P}}\rangle = 0$, where Ψ^{P} is a trial state, and requiring stationarity with respect to the variation of the coefficients $c^N_{\mathcal{R}}$, $\widetilde{c}^B_{\mathcal{R}}$, and $\widetilde{c}^\sigma_{\mathcal{R}}$. This procedure results in the set of equations

$$\begin{aligned} \left(W - M^0_{\mathcal{R}}\right) c^N_{\mathcal{R}}(W) &= V_{N\mathcal{R}}(k_0) + \int \mathrm{d}k\,\frac{V_{N\mathcal{R}}(k)\,\chi^{NN}_{JT}(k,k_0)}{\omega_k + E_N(k) - W} \\ &\quad + \sum_{B'}\int \mathrm{d}k\,\frac{V^{M_{B'}}_{B'\mathcal{R}}(k)\,\widehat{\chi}^{B'N}_{JT}(k,k_0,M_{B'})}{\omega_k + E_{B'}(k) - W} \\ &\quad + \int \mathrm{d}k\,\frac{V^{m_\sigma}_{N\mathcal{R}}(k)\,\widehat{\chi}^{\sigma N}_{JT}(k,k_0,m_\sigma)}{\tilde{\omega}_k + E_{JT}(k) - W}\,, \end{aligned} \tag{11}$$

$$\begin{aligned}
\big(W - M^0_{\mathcal{R}}\big)\,\widehat{c}^{\,B}_{\mathcal{R}}(W,M) \;&=\; V^{M}_{B\mathcal{R}}(k_1) + \int \mathrm{d}k\,\frac{V_{N\mathcal{R}}(k)\,\widehat{\chi}^{NB}_{JT}(k,k_1,M)}{\omega_k + E_N(k) - W} \\
&\quad + \sum_{B'} \int \mathrm{d}k\,\frac{V^{M_{B'}}_{B'\mathcal{R}}(k)\widehat{\chi}^{B'B}_{JT}(k,k_1,M_{B'},M)}{\omega_k + E_{B'}(k) - W} \\
&\quad + \int \mathrm{d}k\,\frac{V^{m_\sigma}_{N\mathcal{R}}(k)\widehat{\chi}^{\sigma B}_{JT}(k,k_1,m_\sigma,M)}{\tilde{\omega}_k + E_{JT}(k) - W}\,, \qquad (12) \\
\big(W - M^0_{\mathcal{R}}\big)\,\widehat{c}^{\,\sigma}_{\mathcal{R}}(W,\mu) \;&=\; V^{\mu}_{\sigma\mathcal{R}}(k_\mu) + \int \mathrm{d}k\,\frac{V_{N\mathcal{R}}(k)\,\widehat{\chi}^{N\sigma}_{JT}(k,k_\mu,\mu)}{\omega_k + E_N(k) - W} \\
&\quad + \sum_{B'} \int \mathrm{d}k\,\frac{V^{M_{B'}}_{B'\mathcal{R}}(k)\,\widehat{\chi}^{B'\sigma}_{JT}(k,k_\mu,M_{B'},\mu)}{\omega_k + E_{B'}(k) - W} \\
&\quad + \int \mathrm{d}k\,\frac{V^{m_\sigma}_{N\mathcal{R}}(k)\,\widehat{\chi}^{\sigma\sigma}_{JT}(k,k_\mu,m_\sigma,\mu)}{\tilde{\omega}_k + E_{JT}(k) - W}\,, \qquad (13)
\end{aligned}$$

where

$$\begin{aligned}
V_{N\mathcal{R}}(k) \;&=\; \langle \Phi_{\mathcal{R}} || V(k) || \Psi_N \rangle = Z_N^{-1/2} \langle \Phi_{\mathcal{R}} || V(k) || \Phi_N \rangle\,, \\
V^{M}_{B\mathcal{R}}(k) \;&=\; \langle \Phi_{\mathcal{R}} || V(k) || \widehat{\Psi}_B(M) \rangle = Z_B^{-1/2} \langle \Phi_{\mathcal{R}} || V(k) || \Phi_B \rangle\,, \\
V^{\mu}_{N\mathcal{R}}(k) \;&=\; \langle \Phi_{\mathcal{R}} || V^\mu(k) || \widehat{\Psi}_N \rangle = Z_N^{-1/2} \langle \Phi_{\mathcal{R}} || V^\mu(k) || \Phi_N \rangle\,.
\end{aligned}$$

Here, Z_B is the wave-function normalization, while the reduced matrix elements $\langle \Phi_{\mathcal{R}} || V(k) || \Phi_N \rangle$ and $\langle \Phi_{\mathcal{R}} || V(k) || \Phi_B \rangle$ are calculated by using the underlying quark model of choice, for instance, the CBM in our sample calculations.

Requiring stationarity with respect to the pion amplitudes leads to the Lippmann–Schwinger equation for the K matrix. The equation for the χ^{NN}_{JT} amplitude, which is related to the elastic part of the K matrix, reads

$$\begin{aligned}
\chi^{NN}_{JT}(k,k_0) \;&=\; \mathcal{K}^{NN}(k,k_0) - \sum_{\mathcal{R}} c^N_{\mathcal{R}}(W) V_{N\mathcal{R}}(k) \\
&\quad + \int \mathrm{d}k'\,\frac{\mathcal{K}^{NN}(k,k')\,\chi^{NN}_{JT}(k',k_0)}{\omega'_k + E_N(k') - W} \\
&\quad + \sum_{B} \int \mathrm{d}k'\,\frac{\mathcal{K}^{NB}_{M_B}(k,k')\,\widehat{\chi}^{BN}_{JT}(k',k_0,M_B)}{\omega'_k + E_B(k') - W} \\
&\quad + \int \mathrm{d}k'\,\frac{\mathcal{K}^{N\sigma}_{m_\sigma}(k,k')\,\widehat{\chi}^{\sigma N}_{JT}(k',k_0,m_\sigma)}{\tilde{\omega}'_k + E_{JT}(k') - W}\,, \qquad (14)
\end{aligned}$$

where we have introduced the kernels

$$\begin{aligned}\mathcal{K}_M^{NB}(k,k') \;=\; &-\sum_{mtm't'} \langle \Psi_N(k)|a^\dagger_{m't'}(k') \\ &\times\left[V^\dagger_{mt}(k)+(\omega_k+E_N(k)-W)a_{mt}(k)\right]\Big|\,\widehat{\Psi}_B(M)\Big\rangle \\ &\times C^{J\frac12}_{J_B\frac12-m'1m'}C^{T\frac12}_{T_B\frac12-t'1t'}C^{J\frac12}_{\frac12\frac12-m1m}C^{T\frac12}_{\frac12\frac12-t1t}\,.\end{aligned}$$

(For $B=N$, $\widehat{\Psi}_B(M)$ reduces to Ψ_N and M to M_N.) The pion amplitudes involving the πB channels, in turn, satisfy the equation

$$\begin{aligned}\widehat{\chi}^{B'B}_{JT}\left(k,k_1,M',M\right) \;=\; &\mathcal{K}^{B'B}_{M'M}(k,k_1)-\sum_{\mathcal{R}}\widehat{c}^{\,B}_{\mathcal{R}}(W,M)V^{M'}_{B'\mathcal{R}}(k) \\ &+\sum_{B''}\int \mathrm{d}k'\,\frac{\mathcal{K}^{B'B''}_{M'M_{B''}}(k,k')\,\widehat{\chi}^{B''B}_{JT}(k',k_1,M_{B''},M)}{\omega'_k+E_{B''}(k')-W} \\ &+\int \mathrm{d}k'\,\frac{\mathcal{K}^{B'\sigma}_{M'm_\sigma}(k,k')\,\widehat{\chi}^{\sigma B}_{JT}(k',k_1,m_\sigma,M)}{\tilde{\omega}'_k+E_{JT}(k')-W}\,, \qquad (15)\end{aligned}$$

with a similar structure of the kernels $\mathcal{K}^{BB'}_{MM'}(k,k')$ and $\mathcal{K}^{B'\sigma}_{M'm_\sigma}$.

Equations (14) and (15), as well as an analogous consideration for the amplitudes involving the σ meson, imply that the pion amplitudes can be written in the following form:

$$\chi^{NN}_{JT}(k,k_0) \;=\; -\sum_{\mathcal{R}} c^N_{\mathcal{R}}(W)\mathcal{V}_{N\mathcal{R}}(k)+\mathcal{D}^{NN}(k,k_0)\,, \qquad (16)$$

$$\widehat{\chi}^{B'B}_{JT}(k,k_1,M',M) \;=\; -\sum_{\mathcal{R}} \widehat{c}^{\,B}_{\mathcal{R}}(W,M)\mathcal{V}^{M'}_{B'\mathcal{R}}(k)+\mathcal{D}^{B'B}_{M'M}(k,k_1)\,, \qquad (17)$$

$$\widehat{\chi}^{B\sigma}_{JT}(k,k_\mu,M,\mu) \;=\; -\sum_{\mathcal{R}} \widehat{c}^{\,\sigma}_{\mathcal{R}}(W,\mu)\mathcal{V}^{M}_{B\mathcal{R}}(k)+\mathcal{D}^{B\sigma}_{M\mu}(k,k_\mu)\,, \qquad (18)$$

$$\widehat{\chi}^{\sigma B}_{JT}(k,k_1,\mu,M) \;=\; -\sum_{\mathcal{R}} \widehat{c}^{\,B}_{\mathcal{R}}(W,M)\mathcal{V}^{\mu}_{\sigma\mathcal{R}}(k)+\mathcal{D}^{\sigma B}_{\mu M}(k,k_1)\,, \qquad (19)$$

$$\widehat{\chi}^{\sigma\sigma}_{JT}(k,k_\mu,\mu',\mu) \;=\; -\sum_{\mathcal{R}} \widehat{c}^{\,\sigma}_{\mathcal{R}}(W,\mu)\mathcal{V}^{\mu'}_{\sigma\mathcal{R}}(k)+\mathcal{D}^{\sigma\sigma}_{\mu'\mu}(k,k_\mu)\,, \qquad (20)$$

where $\mathcal{V}$ are the dressed vertices and $\mathcal{D}$ are the background parts of the amplitudes.

Two simplifications are possible at this point and will be only sketched here. The first one consists in neglecting the terms involving the integrals in Eqs. (11)–(15), resulting in the Born approximation for the K matrix. In

this approximation, the K matrix is constructed from the meson amplitudes (16)–(20) by using Eqs. (9) and (10), and replacing the dressed vertices $\mathcal{V}_{B\mathcal{R}}$ by the corresponding bare vertices $V_{B\mathcal{R}}$, as well as $\mathcal{D}$ by $\mathcal{K}$.

The second simplification is the averaging over invariant masses, for instance, the averaging over the Δ invariant mass M in the $\sigma\Delta$ channel, and invariant mass μ of the two-pion system occurring in the decay of the σ meson. The averaged invariant masses $\bar{M}$ and $\bar{\mu}$ have been found by suitable smooth numerical approximations. Consequently, this type of averaging can be applied to the K matrix and T matrix themselves, and the big advantage of the averaging procedure is that the set of integral Heitler equations (6) becomes a set of algebraic equations.

In the figures below, the results obtained within the Born approximation for the K matrix are shown, but we have also solved the coupled integral equations (11)–(15) beyond Born by introducing further approximations, which have allowed us to write the kernels $\mathcal{K}^{NN}$, $\mathcal{K}^{NB}$, and $\mathcal{K}^{BB'}$ in separable form. The advantage of using separable kernels is immense as one is then able to solve the system exactly. (Since the quark-σ vertex is not as well determined as the quark-π vertex, the σ-meson vertices have only been treated in the Born approximation.)

Finally, we obtain a set of algebraic equations for the coefficients $c^H_{\mathcal{R}}$, where H stands for πN, πB, and σB channels

$$\sum_{\mathcal{R}'} A_{\mathcal{R}\mathcal{R}'}(W) c^H_{\mathcal{R}'}(W, m_H) = b^H_{\mathcal{R}}(m_H)\,,$$

where

$$\begin{aligned}
A_{\mathcal{R}\mathcal{R}'} &= \left(W - M^0_{\mathcal{R}}\right)\delta_{\mathcal{R}\mathcal{R}'} + \sum_{B'} \int \mathrm{d}k\, \frac{\mathcal{V}^{M_{B'}}_{B'\mathcal{R}}(k) V^{M_{B'}}_{B'\mathcal{R}'}(k)}{\omega_k + E_{B'}(k) - W}\,,\\
b^B_{\mathcal{R}} &= V^M_{B\mathcal{R}}(k_1) + \sum_{B'} \int \mathrm{d}k\, \frac{\mathcal{D}^{B'B}_{MM_{B'}}(k, k_1) V^{M_{B'}}_{B'\mathcal{R}}(k)}{\omega_k + E_{B'}(k) - W} = \mathcal{V}^M_{B\mathcal{R}}(k_1)\,,\\
b^\sigma_{\mathcal{R}} &= V^\mu_{N\mathcal{R}}(k_\mu)\,.
\end{aligned}$$

Organizing the coefficients and $\mathcal{V}$ functions into vectors, $\boldsymbol{c}^H = (c^H_{\mathcal{R}}, c^H_{\mathcal{R}'}, \ldots)^T$ and $\boldsymbol{\mathcal{V}}_H = (\mathcal{V}_{H\mathcal{R}}, \mathcal{V}_{H\mathcal{R}'}, \ldots)^T$, the solution can be written in the form $\boldsymbol{c}^H = A^{-1}\boldsymbol{\mathcal{V}}_H$. The zeros of A occur at the positions of the poles of the K matrix related to the resonance $\mathcal{R}$; the corresponding energies are $M_{\mathcal{R}}$. The coefficients $c_{\mathcal{R}}$ have then been determined by the following procedure. First, we have established the zeros of the A-matrix determinant. Second, by adjusting the energies of the bare states, $M^0_{\mathcal{R}}$, the poles of the K matrix have been forced to acquire some desired values. Third, A

has been diagonalized, $UAU^T = D$, such that $D = \mathrm{diag}[\lambda_{\mathcal{R}}, \lambda_{\mathcal{R}'}, \ldots] = \mathrm{diag}[Z_{\mathcal{R}}(W)(W - M_{\mathcal{R}}), Z_{\mathcal{R}'}(W)(W - M_{\mathcal{R}'}), \ldots]$, which defines the wave-function normalization $Z_{\mathcal{R}}$ pertinent to the resonance $\mathcal{R}$. Finally, this allowed the solution for the c coefficients to be cast in the form

$$\boldsymbol{c}^H = U^T D^{-1} U \boldsymbol{\mathcal{V}}_H \,,$$

while the resonant parts of the χ amplitudes take the form

$$\begin{aligned} \chi^{H'H} &= -\boldsymbol{\mathcal{V}}_{H'}^T \boldsymbol{c}^H = -\boldsymbol{\mathcal{V}}_{H'}^T U^T D^{-1} U \boldsymbol{\mathcal{V}}_H \\ &= -\sum_{\mathcal{R}} \widetilde{\mathcal{V}}_{H\mathcal{R}} \frac{1}{Z_{\mathcal{R}}(W)(W - M_{\mathcal{R}})} \widetilde{\mathcal{V}}_{H'\mathcal{R}} = -\sum_{\mathcal{R}} \widetilde{c}_{\mathcal{R}}^H \widetilde{\mathcal{V}}_{H'\mathcal{R}} \,, \end{aligned}$$

where

$$\widetilde{\mathcal{V}}_{H\mathcal{R}} = \sum_{\mathcal{R}'} u_{\mathcal{R}\mathcal{R}'} \mathcal{V}_{H\mathcal{R}'} \,, \qquad \widetilde{c}_{\mathcal{R}}^H = \frac{\widetilde{\mathcal{V}}_{H\mathcal{R}}}{Z_{\mathcal{R}}(W)(W - M_{\mathcal{R}})} \,. \tag{21}$$

The interpretation of (21) is that the resonant states $\mathcal{R}, \mathcal{R}', \ldots$ are not eigenstates of the Hamiltonian and therefore mix

$$\widetilde{\Phi}_{\mathcal{R}} = \sum_{\mathcal{R}'} u_{\mathcal{R}\mathcal{R}'} \Phi_{\mathcal{R}'} \,.$$

In the following, the results for the scattering amplitudes in the P_{11} partial wave are shown. As mentioned above, we have used the CBM as the underlying quark model since it is one of the most popular representations of quark–pion dynamics. Figure 2 (left) shows the real and imaginary parts of the T matrix, and Fig. 2 (right) shows the inelasticity.

Our study has shown that elastic and inelastic pion–nucleon scattering in the energy range from the threshold up to $W \sim 1700$ MeV is governed by an intricate interplay of the πN, $\pi\Delta$, and σN degrees of freedom. In particular, the correlated two-pion decay in the relative s-wave by the σ meson turned out to be the crucial ingredient that allowed us to explain the peculiar feature of the inelasticity in the P_{11} partial wave just above the two-pion threshold, which quickly increases from zero to unity and remains almost constant in a broad energy range. Our findings also imply that one is able to explain the features of the Roper resonance without invoking exotic degrees of freedom, and to establish a specific benchmark for an assessment of the underlying quark models. It would be naive to expect, however, that the scattering analysis alone would be able to provide a definitive criterion for feasible models, so we next turned to the application of the coupled-channel method to full electro-production amplitudes.

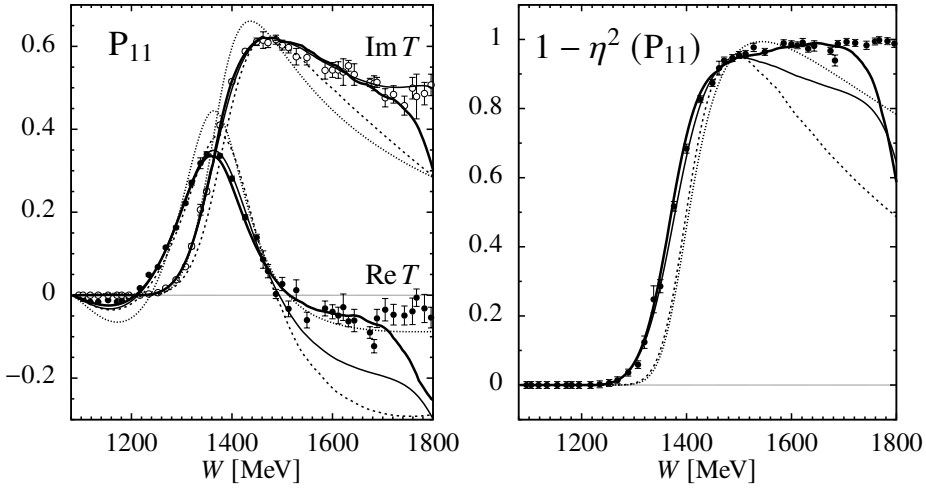

Fig. 2. Left: The real and imaginary parts of the T matrix for the P_{11} partial amplitude. Shown are the Born approximation with resonant terms only (dotted lines), the result including the background (dashed lines), adding the σ channel (thin solid lines), and the full calculation (thick solid lines). Right: The inelasticity in the P_{11} partial wave (the same labeling).

3.1. Calculation of photo- and electro-production amplitudes

Photo- and electro-production have been incorporated into the coupled-channels K-matrix formalism by including a new channel, γN. Since the electro-magnetic interaction is considerably weaker than the strong interaction, we have assumed $K_{\gamma N\,\gamma N} \ll K_{\gamma N\,\pi N} \ll K_{\pi N\,\pi N}$, and similarly for other channels. The electro-magnetic interaction Hamiltonian has been taken in the form

$$H_\gamma = \frac{1}{\sqrt{2\pi}^3} \int \mathrm{d}\vec{k}_\gamma \sum_\mu \left[\tilde{V}_\mu^\gamma \left(\vec{k}_\gamma\right) a_\mu \left(\vec{k}_\gamma\right) + \mathrm{h.c.} \right] ,$$

where $\vec{k}_\gamma$ and μ are the momentum and the polarization of the incident photon, and

$$\tilde{V}_\mu^\gamma \left(\vec{k}_\gamma\right) = \frac{\mathrm{e}_0}{\sqrt{2\omega_\gamma}} \int \mathrm{d}\vec{r}\, \vec{\varepsilon}_\mu \cdot \vec{j}(\vec{r})\, \mathrm{e}^{i\vec{k}_\gamma \cdot \vec{r}} . \tag{22}$$

The K-matrix elements for electro-production corresponding to different channels MB ($\pi N, \pi\Delta$, $\sigma N, \ldots$) are introduced as expectation values of (22) between the state representing the photon–nucleon system, Ψ_N, and the principal-value states,

$$\mathcal{M}_{MB}^{K\,JI} = -\frac{\mathcal{N}_\gamma}{\sqrt{k_0 k_\gamma}} \left\langle \Psi_{JI}^{MB}\,(m_J m_I; k_0, l) \right| \tilde{V}_\mu^\gamma(\vec{k}_\gamma) \left| \Psi_N(m_s m_t) \right\rangle ,$$

where J and I denote spin and isospin, respectively. They are related to the electro-production amplitudes through $\mathcal{M} = \mathcal{M}^K + i\,T\mathcal{M}^K$, a relation that follows from the Heitler equation, Eq. (5). For the P_{11} partial wave in the region of the Roper resonance it turned out that only the $\pi\Delta$ and σN inelastic channels are needed, and we end up with [9]

$$\begin{aligned}\mathcal{M}_{\pi N}(W) \;=\; & \mathcal{M}^K_{\pi N}(W) + i\Bigg[T_{\pi N\pi N}(W)\mathcal{M}^K_{\pi N}(W) \\ & + \int\limits_{M_N+m_\pi}^{W-m_\pi} \mathrm{d}M_\Delta\, T_{\pi N\pi\Delta}(W,M_\Delta)\mathcal{M}^K_{\pi\Delta}(W,M_\Delta) \\ & + \int\limits_{2m_\pi}^{W-M_N} \mathrm{d}\mu\, T_{\pi N\sigma N}(W,\mu)\mathcal{M}^K_{\sigma N}(W,\mu)\Bigg]\,. \end{aligned} \tag{23}$$

Close to a resonance, $\mathcal{R}$ the K-matrix element between the elastic channel and an arbitrary channel MB can be split into the resonant and background parts,

$$K_{\pi N\,MB} = -\pi\sqrt{\frac{\omega_0\omega_M E_N E_B}{k_0 k_M W^2}}\,\tilde{c}^{MB}_{\mathcal{R}}\tilde{\mathcal{V}}^{\pi}_{N\mathcal{R}}(k_0) + K^{\mathrm{bg}}_{\pi N\,MB}\,,$$

and this allows us to split the electro-production amplitudes in the same way: the resonant part takes the form

$$\mathcal{M}^{(\mathrm{res})}_{\pi N} = -\sqrt{\frac{\omega_\gamma E^\gamma_N}{\pi^2\omega_0 E_N}}\,\frac{\sqrt{Z_{\mathcal{R}}}}{\mathcal{V}_{N\mathcal{R}}}\,\left\langle\widehat{\Psi}^{(\mathrm{res})}_{\mathcal{R}}(W)\right|\tilde{V}^\gamma\,|\Psi_N\rangle\;T_{\pi N\pi N}\,,$$

while the background part satisfies

$$\mathcal{M}^{(\mathrm{bg})}_{\pi N} = \mathcal{M}^{K\,(\mathrm{bg})}_{\pi N} + i\left[T_{\pi N\pi N}\mathcal{M}^{K\,(\mathrm{bg})}_{\pi N} + \bar{T}_{\pi N\pi\Delta}\bar{\mathcal{M}}^{K\,(\mathrm{bg})}_{\pi\Delta} + \bar{T}_{\pi N\sigma N}\bar{\mathcal{M}}^{K\,(\mathrm{bg})}_{\sigma N}\right].$$

The remaining steps are the multipole decomposition and calculation of helicity amplitudes. Omitting all details, let us just write down as an illustration a sample relation between the specific electro-production and the helicity amplitude. We obtain

$$\begin{aligned}\mathrm{Im}\,{}_pM^{(1/2)}_{1-} \;=\; & -\frac{1}{3}\sqrt{\frac{k_W E^\gamma_N}{6\pi^2\omega_0 E_N}}\,\frac{\sqrt{Z_{\mathcal{R}}}}{\mathcal{V}^{\pi}_{N\mathcal{R}}}\,\mathrm{Im}T_{\pi N\pi N}\left(-\frac{3}{\sqrt{2}}\right) \\ & \times\left\langle\widehat{\Psi}^{(\mathrm{res})}_{\mathcal{R}}\;\left(m_s=\tfrac{1}{2}\right)\right|\tilde{V}^{M1}\left|\,\Psi_N\;\left(m_s=-\tfrac{1}{2}\right)\right\rangle\,, \end{aligned} \tag{24}$$

where

$$\Gamma_{\pi N} = 2\pi \frac{\omega_0 E_N \mathcal{V}^{\pi}_{N\mathcal{R}}(k_0)^2}{Z_{\mathcal{R}} k_0 W}$$

is the elastic width of the resonance. We thus obtain

$$\mathrm{Im}\, {}_pM^{(1/2)}_{1-} = -\xi_{\mathcal{R}} \sqrt{\frac{k_W E^{\gamma}_N \Gamma_{\pi N}}{6\pi k_0 M_{\mathcal{R}} \Gamma^2}}\; A^p_{1/2}\,.$$

Phenomenological studies of electro-production reveal a relatively strong contribution of the ω meson already at low energies, whereas in the calculation of the (strong) scattering amplitudes, the contributions of vector mesons are negligible. The contribution of the ω meson to the K matrix in the elastic channel has therefore been modeled by the expression

$${}_pM^{(1/2)}_{1-}(\omega{-}\mathrm{meson}) = \frac{1}{3}\,\frac{M_N}{4\pi W m_\pi}\,\frac{g_{\gamma\pi\omega} g_{\omega 1}\, k_\gamma k_\pi\, \rho_\omega(k_\omega)}{m^2_\omega - m^2_\pi + 2k_\gamma \omega_\pi}\,,$$

where $\rho_\omega(k_\omega)$ is the appropriate form-factor; see [9] for details.

Figure 3 shows a sample result for the ${}_pM^{(1/2)}_{1-}$ amplitude by using the same parameters for the CBM model as in the calculation of the scattering amplitudes. One of the more interesting findings in the P_{11} case was that

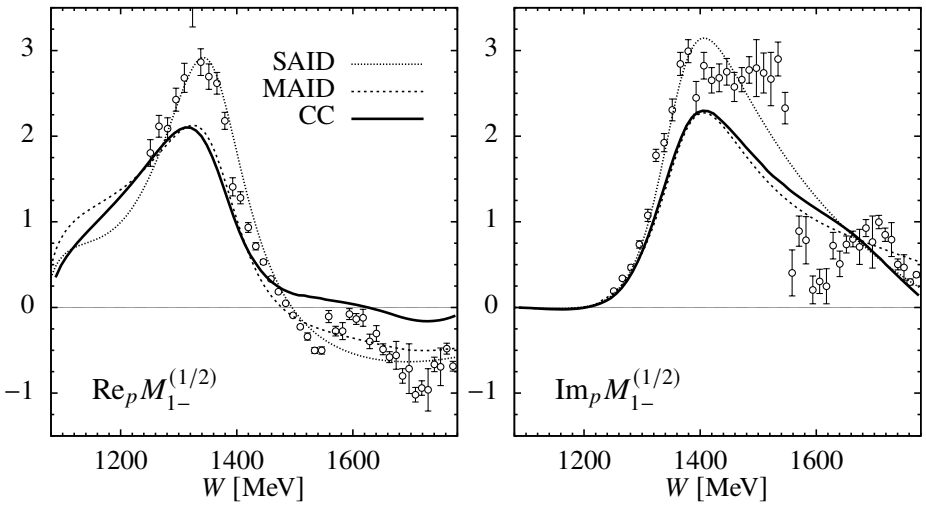

Fig. 3. Real (left) and imaginary (right) part (see Eq. (24)) of the ${}_pM^{(1/2)}_{1-}$ photoproduction amplitude. The experimental points are the single-energy solutions of the SAID partial-wave analysis [10, 11]; the "SAID" curve shows the corresponding fit; the MAID result is based on the parametrization provided by [12].

at energies below the resonance, the amplitudes are dominated by the background, which is marked in contrast to the P_{33} partial wave in the region of the $\Delta(1232)$, where the photo-production amplitude is clearly dominated by the resonant contribution and follows the shape of the elastic T matrix.

As a further example, Fig. 4 shows the scalar helicity amplitude, evaluated at $W = 1520$ MeV, the pole of the K matrix. We observed an interesting feature that the effects of the pion cloud which, understandably, are most pronounced at small Q^2, have the opposite sign with respect to the contribution from the quark core, which is small at the origin — with the same mechanism also governing the behavior of the magnetic helicity amplitude (not shown). The large spread of various quark-model predictions for the scalar helicity amplitude near the real-photon point and the uncertainties of the helicity couplings $S^p_{1/2}(0)$ found by SAID and MAID motivated us for an experimental exploration mentioned in Section 4.

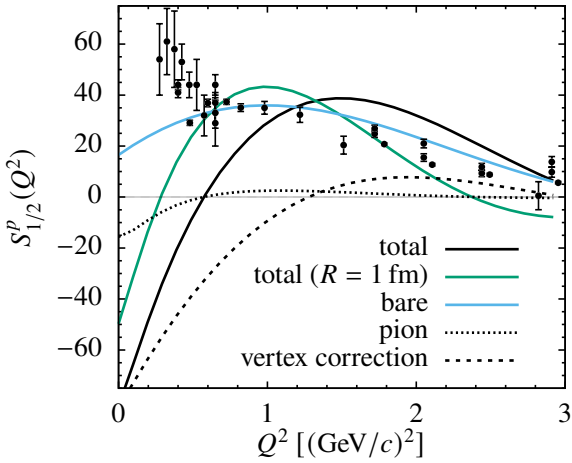

Fig. 4. Scalar helicity amplitude $S^p_{1/2}(Q^2)$ evaluated at the pole of the K matrix ($W = 1520$ MeV). Separately shown are the contributions of the $3q$ core ("bare"), the $\gamma\pi\pi'$ interaction ("pion"), and the pion-cloud corrections to the $\gamma BB'$ vertex correction ("vertex"). An additional "total" curve is plotted for a non-standard bag radius of 1 fm (otherwise 0.83 fm).

3.2. Including the "second Roper"

An additional impetus to investigate the structure of the Roper resonance came as part of a larger enterprise to study eta and kaon photo-production on nucleons within the same coupled-channel approach as described above. The required energy range necessarily extended up to $\approx$ 1800 MeV, and this naturally led to the inclusion of the "second Roper", the $N^*(1710)$, for which we assumed that it decays only into the σN channel. Furthermore,

the production of strange mesons in the P_{11} partial wave required us to specify its quark configuration, which is not obvious; it may consist of the $(1s)^3$, $(1s)^2(2s)^1$, $(1s)^1(2s)^2$, $(1s)^1(1p)^2$, $(1s)^1(1d)^2\ldots$ configurations or even a component with the excitation of the σ cloud [4]. We have restricted our investigation to the type of excitation in which only a single $1s$ quark is promoted to a higher orbit, which resulted in the following structure of the two Roper resonances [13]:

$$\begin{aligned} N^*(1440) &= \cos\vartheta_R(1s)^2(2s)^1 - \sin\vartheta_R(1s)^1(1x)^2\,, \\ N^*(1710) &= \sin\vartheta_R(1s)^2(2s)^1 + \cos\vartheta_R(1s)^1(1x)^2\,. \end{aligned}$$

Here, x stands for $l > 0$ quark orbits not involved in the transition matrix elements. Note that the $N^*(1440)$ and the ground state also mix, which leads to an important nucleon–pole contribution to the amplitudes.

3.3. Genuine quark state versus dynamically generated structure

Our last theoretical effort was motivated by the recent lattice QCD studies (Graz, Adelaide) that have found no clear signal for a dominant three-quark configuration below 1.65 GeV and 2.0 GeV, respectively, that could be interpreted as a Roper state. It seemed that the πN channel alone does not render a low-lying resonance and that coupling with $\pi\pi N$ channels seems to be important, supporting the dynamical origin of the Roper. With our coupled-channels machinery in place, we decided to investigate whether such a dynamical mechanism for the formation of the Roper would be possible. This work has been performed in collaboration with Tuzla (H. Osmanović) and Zagreb (A. Švarc) groups [14].

The pion–baryon vertices in the underlying quark model (still CBM) have been fixed, while the s-wave sigma-baryon interaction has been incorporated phenomenologically with the coupling strength, the mass, and the width of the σ meson introduced as free parameters. The Laurent–Pietarinen expansion has been used to extract the parameters of the S-matrix pole. The Lippmann–Schwinger equation for the K matrix with a separable kernel has been solved to all orders. The main finding was that for sufficiently strong σNN coupling, the kernel becomes singular and a quasi-bound state emerges at around 1.4 GeV, dominated by the σN component and manifesting itself as a pole of the S matrix. As an alternative, we have added a $(1s)^2 2s$ quark resonant state, and studied the interplay of the dynamically generated state and the three-quark resonant state. It turned out that for the mass of the three-quark resonant state above 1.6 GeV, the mass of the resonance is indeed determined solely by the dynamically generated state, yet with the caveat that the three-quark resonant state remains imperative to reproduce the experimental width and the modulus of the resonance pole.

4. Experimental studies of the Roper resonance

The Ljubljana group also led an experimental effort within the A1 Collaboration at the MAMI facility. We have precisely measured the proton recoil polarization components in the $p(\vec{e}, e'\vec{p})\pi^0$ process in the energy range of the Roper resonance and, by using the MAID unitary isobar model, have been able to determine (in a model-dependent manner) the scalar helicity amplitude $S_{1/2}$ at a Q^2 very close to the real-photon point [15]. In view of the cancellations of bare-core and pion–cloud contributions seen by some models at low Q^2, this region is relevant as a kind of "elimination ground" for quark models. Our extracted value (see Fig. 5) is consistent with the non-hybrid nature of the resonance, which implies that the interpretations of the Roper as an entity characterized by strong meson–baryon dressing may be favored, in other words, there is no need for non-quark degrees of freedom. Our result, therefore, supports those models of the Roper in which the interplay of quark and meson contributions results in a small value of $S_{1/2}$ near the real-photon point.

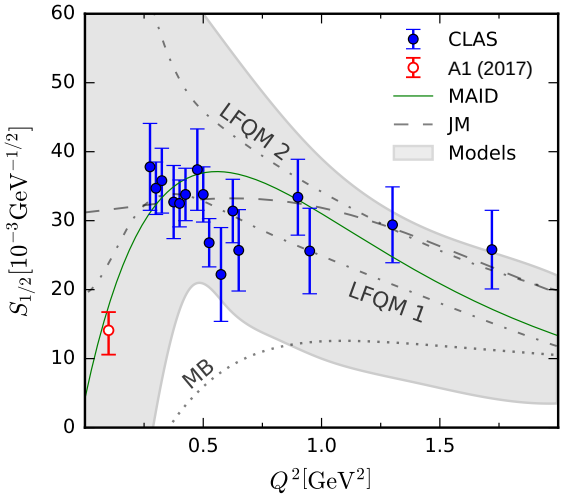

Fig. 5. The scalar helicity amplitude for Roper electro-excitation at $Q^2 = 0.1$ $(\mathrm{GeV}/c)^2$, denoted "A1 (2017)", compared to CLAS data, MAID, the JLab-MSU parametrization, and two light-front quark model results. The "MB" curve shows the meson–baryon dressing contribution. The immense range of various model predictions is indicated by shading; see [15] for detailed references.

With this paper, the Author would like to pay tribute to the late Professor Bojan Golli, who for many years was the driving force in nucleon resonance-related theoretical efforts of the Ljubljana group.

REFERENCES

[1] L.D. Roper, «Evidence for a P_{11} Pion–Nucleon Resonance at 556 MeV», *Phys. Rev. Lett.* **12**, 340 (1964).

[2] L. Alvarez-Ruso, «On the nature of the Roper resonance», in: B. Golli, M. Rosina, S. Širca (Eds.) «Proceedings of the Mini-Workshop Dressing Hadrons», Bled, Slovenia, 4–11 July, 2010, pp. 1–8.

[3] J. da Providência, J. Urbano, «Pion–nucleon resonances and the Peierls–Yoccoz projection», *Phys. Rev. D* **18**, 4208 (1978).

[4] P. Alberto, M. Fiolhais, B. Golli, J. Marques, «N^* electroproduction amplitudes in a model with dynamical confinement», *Phys. Lett. B* **523**, 273 (2001).

[5] M. Fiolhais, B. Golli, M. Rosina, S. Širca, «Counting pions in the nucleon», *Prog. Part. Nucl. Phys.* **36**, 151 (1996).

[6] I. Aznauryan, V. Burkert, «Electroexcitation of nucleon resonances», *Prog. Part. Nucl. Phys.* **67**, 1 (2012).

[7] B. Golli, S. Širca, «Roper resonances in chiral quark models», *Eur. Phys. J. A* **38**, 271 (2008).

[8] G.F. Chew, F.E. Low, «Effective-Range Approach to the Low-Energy p-Wave Pion–Nucleon Interaction», *Phys. Rev.* **101**, 1570 (1956).

[9] B. Golli, S. Širca, M. Fiolhais, «Pion electro-production in the Roper region in chiral quark models», *Eur. Phys. J. A* **42**, 185 (2009).

[10] R.A. Arndt, I.I. Strakovsky, R.L. Workman, M.M. Pavan, «Updated analysis of πN elastic scattering data to 2.1 GeV: The baryon spectrum», *Phys. Rev. C* **52**, 2120 (1995).

[11] R.A. Arndt *et al.*, «Dispersion relation constrained partial wave analysis of πN elastic and $\pi N \to \eta N$ scattering data: The baryon spectrum», *Phys. Rev. C* **69**, 035213 (2004).

[12] D. Drechsel, S.S. Kamalov, L. Tiator, «Unitary isobar model — MAID2007», *Eur. Phys. J. A* **34**, 69 (2007).

[13] B. Golli, S. Širca, «Eta and kaon production in a chiral quark model», *Eur. Phys. J. A* **52**, 279 (2016).

[14] B. Golli, H. Osmanović, S. Širca, A. Švarc, «Genuine quark state *versus* dynamically generated structure for the Roper resonance», *Phys. Rev. C* **97**, 035204 (2018).

[15] A1 Collaboration (S. Štajner *et al.*) , «Beam-Recoil Polarization Measurement of π^0 Electroproduction on the Proton in the Region of the Roper Resonance», *Phys. Rev. Lett.* **119**, 022001 (2017).